Hindawi
Journal of Sensors
Volume 2023, Article ID 5569714, 14 pages
https://doi.org/10.1155/2023/5569714

Research Article

Weak Sinusoidal Signal Detection with CSI Model in Chaotic Interference

Liyun Su,[1,2] **Wanlin Zhu**,[1] **Fenglan Li**,[3] **and Chunquan Pan**[1]

[1]*School of Science, Chongqing University of Technology, Chongqing 400054, China*
[2]*Center for Spatio-Temporal Big Data Research, Chongqing University of Technology, Chongqing 400054, China*
[3]*Library, Chongqing University of Technology, Chongqing 400054, China*

Correspondence should be addressed to Liyun Su; cloudhopping@163.com

Received 25 July 2023; Revised 12 November 2023; Accepted 27 November 2023; Published 14 December 2023

Academic Editor: Rajkishor Kumar

In small target detection under strong sea clutter or impact signal detection under machinery fault diagnosis, a weak sinusoidal signal with random amplitude is often contaminated by heavier chaotic noise, and the target information is difficult to detect. Traditional solutions, such as neural networks or stochastic resonance, can not effectively extract heteroscedasticity of data, which leads to weak signals not being detected. To overcome these limitations and improve the detection efficiency, an empirical likelihood ratio statistical method for detecting weak sinusoidal signals with random amplitude under strong chaotic interference is proposed. First, based on the reconstruction in the phase space of the 1-D observed time series signal with embedding dimension and time delay, the presented method obtains a multivariate special temporal series as an input. Subsequently, the chaotic single index (CSI) statistical model is established for single-step prediction, and it can be estimated by the nonparametric locally linear algorithm for minimizing the mean squares error. Finally, the empirical likelihood ratio statistical method is applied to detect weak sinusoidal signals with random amplitude. Simulated data and real data experiment results show that the proposed CSI model can better capture the weak target signal and detect effectively weak target signal under the chaotic interference.

1. Introduction

Weak signal detection or anomaly detection are essential and critical tasks in machine monitoring, sea cluster target detection, and fault diagnosis for many modern intelligent systems [1–3]. The emergence of weak target signals during operation or monitoring indicates a fault or dangerous situation [4–6] and leads to enormous economic loss and safety issues. Therefore, effective and highly accurate weak signal detection techniques can be studied and developed. Based on the traditional method, the weak signal under chaotic background is generally not easy to detect. A weak target signal is relatively low compared to noise. It not only says that the amplitude of the detected signal is small but also mainly refers to the targeted signal that is submerged by strong noise and has a low signal-to-noise ratio (SNR). Current methods for detecting weak signal research fields are statistical method [7, 8], Duffing oscillator method [9–11], stochastic resonance method [12–14], Elman neural network [15], deep learning models [16], or broad learning [17, 18], etc. Su et al. [7] presented statistical detection and extraction models with phase threshold autoregressive (PTAR) model and double layer threshold autoregressive model in chaotic noise, based on the PTAR, pulse linear form, Markov chain Monte Carlo, and profile least squares algorithm. Zhihong and Shaopu [9] proposed a weak signal detection method based on the Van Der Pol–Duffing oscillator and a weak signal is detected through the transition from the chaotic to the periodic state. Silva et al. [12] applied stochastic resonance for a weak periodic signal in the chaotic systems. Su et al. [15] established Elman deep learning adaptive detection model for weak pulse signal detection and used a hypothesis test to detect weak pulse signals from the prediction error. However, despite several enhancements and renewals in the domain of intelligent signal processing, such approaches involve certain limitations and deficiencies, especially for weak signal detection submerged in the chaotic interference.

A sinusoidal signal is a common signal in the fields of chaotic secure communication, rotating machinery fault diagnosis, and oscillating circuits, and is often interfered with by the Gaussian white noise and chaotic noise. Effective detection of weak sinusoidal signals submerged by chaotic background noise is the basis for reducing the cost of testing equipment and developing high-precision testing instruments. It has important theoretical and practical significance. The detection of weak sinusoidal signals under chaotic noise has become a hot topic in the academic circles. Su et al. [19] proposed a local linear Periodic–Kalman filtering hybrid algorithm to detect weak signals. Maoiléidigh and Hudspeth [20] described the detection of sinusoidal signals by noisy supercritical and subcritical Hopf oscillators; Luo et al. [21] proposed a nonautonomous chaotic oscillator for estimating the amplitude of weak eigenvalue signals at different frequencies. These methods have achieved certain effects, but the chaotic noise background cannot be completely removed, it is susceptible to the white noise interference, and the adaptability is not strong. Sharifi-Tehrani et al. [22–24] use the properties of eigen-space and eigen-spectrum of symmetric and Toeplitz covariance matrix, to address the problem of detecting/estimating very low-SNR sinusoidal signals. Su et al. [25] aimed at the problem of insufficient detecting capacity for weak harmonic signals under chaotic interference, an empirical likelihood ratio method for detecting weak harmonic signals is proposed, but this paper introduced a chaotic linear model, which is inadequate for fitting and detecting weak signals under the chaotic background because of the nonlinearity and complexity of the 1-D received data.

This study is inspired by the locally linear nonparametric techniques and the empirical likelihood ratio statistical model in heteroscedasticity and sequence correlation tests, among other fields. To improve the ability of the sinusoidal signals detection with random amplitude in the background of strong chaotic noise, this study proposes an empirical likelihood ratio statistical method for detecting weak sinusoidal signals with random amplitude under strong chaotic background. The proposed method can obtain reasonable parameter estimation through a locally linear fitting for multidimensional spatio–temporal reconstructing data and reduce the detection error required for weak target signals.

The major innovative contributions of our investigation can be summarized as follows:

(1) A novel chaotic single index (CSI) statistical model with phase space reconstructing is established and its parameters are estimated by a locally linear nonparametric algorithm. This study represents the first effort to develop a chaotic single index architecture for weak signal detection, with the most optimal improvements to handle multidimensional reconstructing data. Compared with the BP neural networks, the model for detecting weak signals under chaotic noise inherits the excellent properties of low-computing load and high-prediction accuracy and avoids the curse of dimensionality.

(2) The empirical likelihood ratio function is further constructed for detecting hypothesis problems. We creatively turn the heteroscedasticity test of a single index model into weak signal detection under chaotic interference. Additionally, the Lagrange multiplier technique is applied to solve the empirical likelihood ratio function and its parameter optimization is realized by using the sequential quadratic programing (SQP) algorithm.

(3) The proposed scheme can detect weak sinusoidal signals submerged in chaotic noise under different conditions and scenarios. An R statistic is investigated for the system parameters and is compared with chi-square values to discriminate the existence of a weak sinusoidal signal of random amplitude.

The rest of the article is arranged as follows: Section 2 introduces the problem analysis of sine signal detection. Section 3 establishes the proposed CSI model and describes the contour empirical likelihood ratio detection of weak sinusoidal signals. Section 4 completes the numerical simulation and analysis. Finally, Section 5 gives the conclusion.

2. Problem Analysis for Sinusoidal Signal Detection

Because chaotic background noise is a strong interference for the sinusoidal signal with random amplitude, if the observation 1-D signal is directly applied to judge the existence of the detected weak signal, its complexity and chaotic nonlinearity are difficult to be described or fit and the existence of a weak sinusoidal signal with random amplitude is hard to be captured. Therefore, the detection scheme in this study is proposed by using the single index model with phase space reconstruction.

From a statistical perspective, the detection of a weak target signal in the strong background of chaotic interference can be described as the following binary hypothesis testing problem:

$$\begin{aligned} H_0 &: y(t) = w(t) + n(t) \\ H_1 &: y(t) = w(t) + s(t) + n(t), \end{aligned} \tag{1}$$

where $y(t)$ represents the original received 1-D data signal, $w(t)$ represents the strong chaotic interference background, $s(t)$ represents the useful target signal and is independent of the chaotic interference, and $n(t)$ represents the Gaussian white noise with a mean of zero. From this general description of the null hypothesis and the alternative hypothesis, we can understand that the alternative hypothesis implies the existence of useful information. As shown in Figure 1, in order to better explain the weak sinusoidal signal with random amplitude under strong chaotic noise, lorenz is used to generate $w(t)$, $s(t)$, $n(t)$, and $y(t)$, where $w(t)$ generates 4,000 points of data for using lorenz without noise; $s(t)$ is the data of 4,000 points generated by Equation (17); $n(t)$ is the white noise data of 4,000 points with a mean value of 0 and a variance of 0.05; $y(t)$ is the sum of $w(t)$, $s(t)$, and $n(t)$.

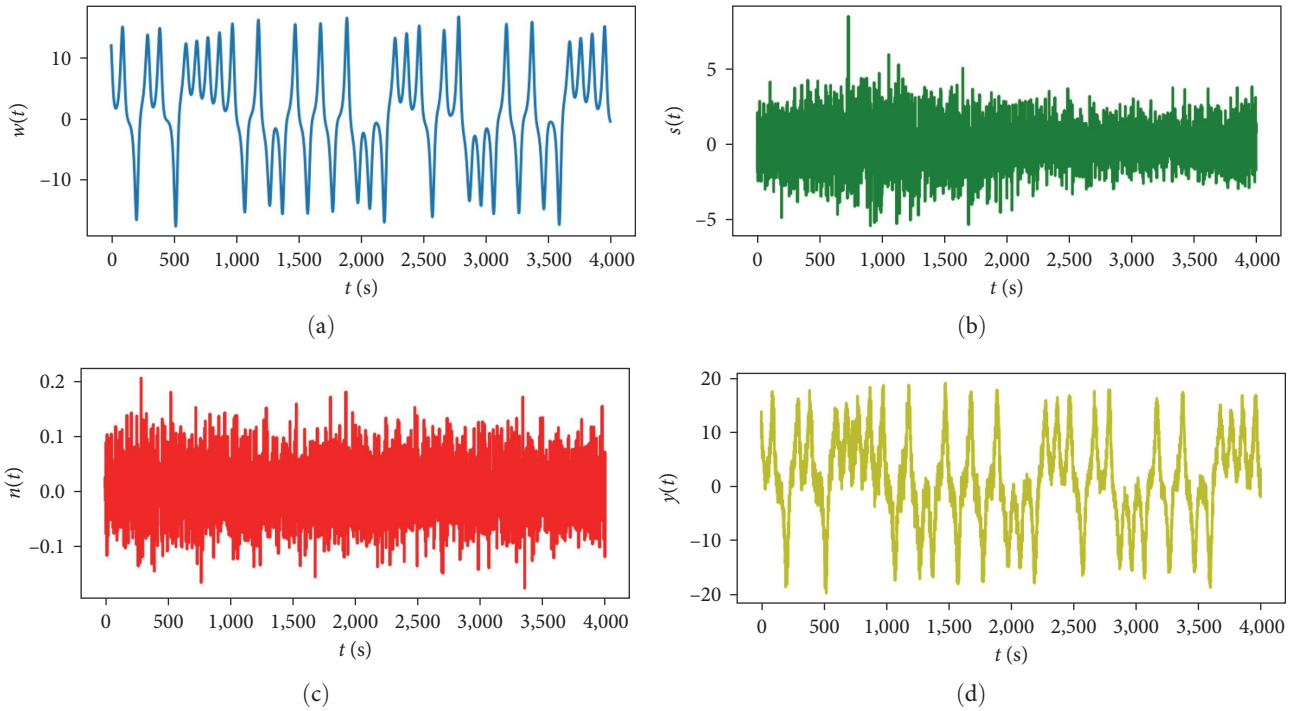

FIGURE 1: All lorenz signal graphs: (a) $w(t)$ of 4,000 points; (b) $s(t)$ of 4,000 points; (c) $n(t)$ with a mean of 0 and a variance of 0.05 at 4,000 points; (d) $y(t)$ of 4,000 points.

Because the strong chaotic interference masks the weak useful information, the above can not be directly applied for the existence detecting. Therefore, the strong chaotic interference should be fitted statistically and suppressed. So the observation signal can be modeled with a single index statistical model, and the target signal can be obtained by subtraction. Therefore, the above hypothesis test problem can be changed into the following form:

$$\begin{aligned} H_0^- &: y(t) - w(t) = n(t) \\ H_1^- &: y(t) - w(t) = s(t) + n(t), \end{aligned} \tag{2}$$

when H_0^- is true, the variance $\mathrm{Var}(y(t) - w(t))$ (i.e., σ^2) is a constant. When H_1^- is true, σ^2 is a time-varying function, so the weak random amplitude sinusoidal signal detection under a strong chaotic noise can be transformed into the following statistical hypothesis testing questions:

$$\begin{aligned} H_0^1 &: \sigma^2 = \sigma_0^2 \\ H_1^1 &: \sigma^2 \neq \sigma_0^2, \end{aligned} \tag{3}$$

where σ_0^2 is a constant, which is the variance of white noise $n(t)$. If the null hypothesis is true, the random amplitude sinusoidal signal in the received 1-D data do not exist; if the alternative hypothesis is true, the random amplitude weak sinusoidal signal in the strong chaotic 1-D data exists.

3. Methods

Equation (2) indicates that the strong chaotic interference should be fitted and removed first, subsequently, the prior knowledge about the chaotic complexity and nonlinearity of the background can be applied to reconstruct a size-fixed tuple in the phase space of the 1-D observed data and the CSI scheme is established to fit the strong chaotic interference. Then the empirical likelihood ratio is used to detect the weak sinusoidal signal of CSI fitting results.

In this section, the specific flowchart is shown in Figure 2, in which "signal prediction" means that the input data containing chaotic noise, white noise, and weak sinusoidal signal are reconstructed in phase space, and then the reconstructed sequence is built into a chaotic single exponential model for one-step prediction, and is estimated by a nonparametric local linear algorithm that minimizes the mean square error (MSE). The "signal detection" part shows that the estimation equation obtained by CSI model is used to test the target signal by empirical likelihood ratio statistics.

3.1. Proposed CSI Model. We creatively utilize CSI regression to construct a novel hybrid model with the empirical likelihood ratio technique and local linear expansion for weak signal detection under chaotic interference, namely, CSI. In order to make it fully suitable for processing 1-D time series signal data, phase space reconstruction is applied to the architecture.

3.1.1. Reconstructing a Phase Space Multidimensional Input Signal. For the observed 1-D data $\{y(t), t = 1, 2, \cdots, \Gamma\}$, where Γ is the sample size, a phase vector in the reconstructed phase space can be interpreted as follows:

$$Y(t) = (y(t), y(t-\tau), \cdots, y(t-(m-1)\tau)), \tag{4}$$

where $t = n_1, n_1 + 1, \cdots, \Gamma, n_1 = 1 + (m-1)\tau$. Reconstruct the original input one-dimension into M-dimension. Takens'

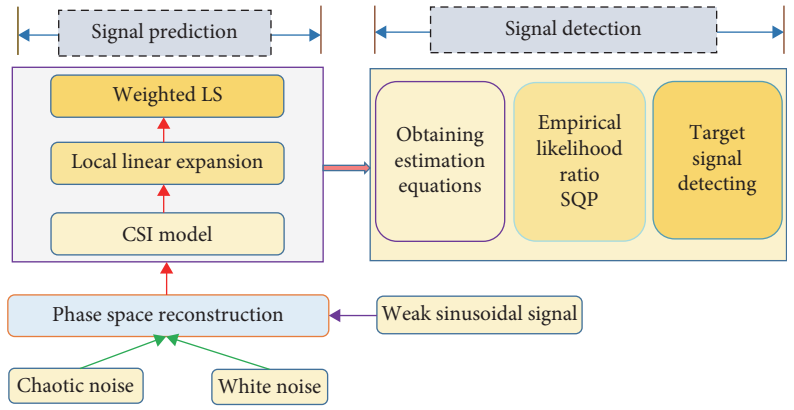

FIGURE 2: The overall architecture of the weak sinusoidal target detection in the chaotic interference.

theorem indicates that for each vector in the reconstructed phase space trajectory, there is a smooth map $f: R^m \longrightarrow R$, such that: $y(t+1) = f(Y(t))$, where $t = n_1, n_1+1, \cdots, \Gamma - 1$. For convenience, t is recoded to $t = 1, 2\cdots, n$. If the f can be found or the approximate mapping $\widehat{f}$ of f is found, the next data point $y(t+1)$ can be predicted. In this study, the delay time τ is computed by the mutual information function method, and the embedded dimension is obtained by the Cao's [26] method.

3.1.2. Chaotic Single Index Statistical Model (CSI Model). After reconstructing the phase space, the semiparametric CSI model for multidimensional input data is established to approximate the mapping f as follows:

$$y(t+1) \approx f(Y(t)), \tag{5}$$

$$f(Y(t)) = g(\beta^T Y(t)) + \varepsilon(t), \tag{6}$$

where $g(\cdot)$ is an unknown catenation function and β is a vector of unknown m-dimensional parameters, $\varepsilon(t) \sim N(0, \sigma_1^2)$ is the model error with independent and identical distribution and has zero mathematical expectations. Profile least squares estimation is conducted with local linearity technique to estimate the smooth unknown function $g(\cdot)$ in the mapping Equation (6) and then proceed to the next step, for point $\beta^T Y(t)$ in some little neighboring domain of u, which is an interest grid point, we use an element-wise locally linear function:

$$\begin{aligned} g(\beta^T Y(t)) &= g(u) + g'(u)(\beta^T Y(t) - u) \\ &= a_0 + a_1(\beta^T Y(t) - u). \end{aligned} \tag{7}$$

Approaching $g(\cdot)$, where $a_0 = g(u), a_1 = g'(u)$. So we have:

$$g(\beta^T Y(t)) = a_0 + a_1(\beta^T Y(t) - u). \tag{8}$$

Let $K(\cdot)$ be a Gaussian smooth kernel function and adjust the weight of each neighbor by changing the window width $h = h_n > 0$. $K_h(\cdot) = K(\cdot/h)/h$. Minimize the objective function for any fixed point β:

$$\begin{aligned} L(a_0, a_1) = \sum_{t=1}^{n} \{&[y(t+1) - a_0 - a_1(\beta^T Y(t) - u)]^2 \\ &\cdot K_h(\beta^T Y(t) - u)\}. \end{aligned} \tag{9}$$

We can obtain the optimal minimum estimation of point $\widehat{a}_0$, $\widehat{a}_1$. Therefore, a locally linear element-wise estimate of $g(\cdot)$ is $\widehat{g}(u;\beta) = \widehat{a}_0$, $g'(u,\beta) = \widehat{a}_1$. The estimated amount is lower than the convergence speed of $\widehat{g}$. If $\widehat{g}'$ and $\widehat{g}$ use the same bandwidth, and it will cause the convergence rate of β's estimator $\widehat{\beta}$ to be lower than $\sqrt{n}$, thus it affects the progressive normality of $\widehat{\beta}$. Consequently, another bandwidth is used for $\widehat{g}'$. It can be introduced by the weighted least squares theory (weighted LS) as follows:

$$\widehat{a}_0 = \sum_{t=1}^{n} w_t(u,\beta) y(t+1), \tag{10}$$

$$\widehat{a}_1 = \sum_{t=1}^{n} \overline{w}\,(u,\beta) y(t+1), \tag{11}$$

with

$$w_t(u,\beta) = \frac{K_h(\beta^T Y(t) - u) \cdot \left[S_{n,2} - (\beta^T Y(t) - u) S_{n,1}\right]}{n\left(S_{n,0} S_{n,2} - S_{n,1}^2\right)}, \tag{12}$$

$$\overline{w}\,(u,\beta) = \frac{K_{h_1}(\beta^T Y(t) - u) \cdot \left[(\beta^T Y(t) - u) S_{n,0} - S_{n,1}\right]}{n\left(S_{n,0} S_{n,2} - S_{n,1}^2\right)}, \tag{13}$$

$$S_{n,l} = \frac{1}{n} \sum_{t=1}^{n} (\beta^T Y(t) - u)^l K_h(\beta^T Y(t) - u), \; l = 0, 1, 2. \tag{14}$$

Substituting the estimated values of a_0 and a_1 into Equation (9) and finding the minimum value of the objective

function, the weighted least squares theory can be derived as follows:

$$\beta = (X^T W X)^{-1} X^T W y, \tag{15}$$

where $X = \widehat{a}_1 Y(t), W$ is the diagonal matrix produced by $K_h(\beta^T Y(t) - u), y = y(t+1) - \widehat{a}_0 + \widehat{a}_1 u$. Equations (10), (11), and (15) are repeated in this way until the three parameters a_0, a_1, and β are stable and convergent, and ultimately the optimal solution of a_0, a_1, and β. Substituting $\widehat{a}_o, \widehat{a}_1$, and $\widehat{\beta}^T$ into Equation (8) yields a one-step predicted value $g(\beta^T Y(t))$, which is then substituted into Equation (6) to obtain a CSI model. Furthermore, this yields prediction errors for the sake of weak signal detection processing as follows:

$$e(t+1) = y(t+1) - g(\beta^T Y(t)). \tag{16}$$

Then, the prediction error contains only a weak sinusoidal signal and white noise theoretically, and since the variance of the random amplitude sinusoidal signal is time-varying and the white noise variance is fixed. Therefore, the approach based on the profile empirical likelihood ratio for the CSI model can be certainly applied to test whether the prediction residual has heteroscedasticity, thereby detecting a random amplitude sinusoidal signal in strong chaotic noise.

3.2. Profile Empirical Likelihood Ratio Detection for Weak Sinusoidal Signal. Equation (3) indicates that the testing of the random amplitude sinusoidal signal in the chaotic interference is equivalent to testing the heteroscedasticity of the prediction residual. The profile empirical likelihood ratio approach is effective for testing heteroscedasticity, thus an empirical likelihood ratio method is investigated. In this section: (1) a sinusoidal signal detection model with random amplitude under chaotic noise, namely, the CSI scheme, is proposed; (2) a method of detecting random amplitude sinusoidal signals based on profile empirical likelihood ratio is developed; (3) a flowchart framework and the pseudocode for detecting sinusoidal signal with random amplitude underthe chaotic interference are designed.

This paper comprehensively studies the detection of weak sinusoidal signals with random amplitude in chaotic noise. The infra sound signal of debris flow is a signal with a typical sinusoidal waveform and amplitude of vibration as a function of energy. Suppose this signal can be expressed as follows:

$$s(t) = d \cdot V \cdot \sin(2\pi f_0 t), \tag{17}$$

where V obeys the standard normal distribution, d controls the amplitude of the sinusoidal signal, f_0 is the frequency of the sinusoidal signal, and t represents time. $s(t)$ is an independent random variable subject to a normal distribution, satisfying: $E(s(t)) = 0, \mathrm{Var}(s(t)) = (d \cdot \sin(2\pi f_0 t))^2 \widehat{=} m(t, d)$. The sinusoidal signal detection model with random amplitude can be further transformed into the following statistical hypothesis test problem:

$$H_0^2 : \mathrm{Var}(\varepsilon(t)) = \sigma_0^2 \quad \text{vs.} \quad H_1^2 : \mathrm{Var}(\varepsilon(t)) = m(t, d) + \sigma_0^2. \tag{18}$$

If $m(t, d) = 0$, the sinusoidal signal of random amplitude does not have heteroscedasticity, there is no weak sinusoidal signal of random amplitude. If $m(t, d) \neq 0$, the sinusoidal signal of random amplitude necessarily has heteroscedasticity, because $m(t, d)$ is a function of changing with time t, there is a weak sinusoidal signal of random amplitude. Therefore, the profile empirical likelihood ratio method can be used to check whether the variance of sinusoidal signals of random amplitude is always equal to zero.

3.2.1. Proposed Empirical Likelihood Ratio Detection Method. First, we apply the empirical likelihood ratio [27–29] to develop a novel detection approach with the CSI model for weak signal detection under chaotic noise. The CSI model established in the previous section:

$$y(t+1) = g(\beta^T Y(t)) + \varepsilon(t). \tag{19}$$

Only the chaotic noise interference is fitted and $\varepsilon(t)$ mainly contains $s(t)$ and $n(t)$. The presence or absence of a sinusoidal signal that determines a random amplitude depends on whether it is $m(t, d) = 0$. In the specific form of $m(t, d)$ proposed in this paper, there is a specific $d^* = 0$ so that $m(t, d^*) = 0$ is true for all t. Therefore, testing the absence or presence of a weak sinusoidal signal with a random amplitude is equivalent to testing the hypothesis test problem below:

$$H_0^3 : d = d^* \quad \text{vs.} \quad H_1^3 : d \neq d^*. \tag{20}$$

To construct the empirical likelihood ratio, the estimation is first obtained as follows:

$$\varepsilon(t) = y(t+1) - g(\beta^T Y(t)). \tag{21}$$

From $E(\varepsilon(t)) = 0$, the following estimation Equation (22) is obtained:

$$\begin{cases} L_{1t} = (\dot{m}^T, 1)^T [(y(t+1) - g(\beta^T Y(t)))^2 - \sigma^2] \\ L_{2t} = D[y(t+1) - g(\beta^T Y(t))] \end{cases}. \tag{22}$$

Let the variance of $\varepsilon(t)$ be an estimate of σ^2, $\dot{m}$ denote the dth derivative of $m(t, d)$ with respect to the null hypothesis, D denote the derivative of $g(\beta^T Y(t))$ with respect to β^T, $L_t = (L^T{}_{1t}, L^T{}_{2t})^T$ is a $(m + q + 1) \times 1$-dimensional vector, and q denotes the dimension of $m(t, d)$. Because under the null hypothesis, $\dot{m}^T$ is a zero vector, so:

$$E(L_{1t}) = E\left(\frac{1}{n}\sum_{t=1}^{n}(\dot{m}^T, 1)^T[(y(t+1) - g(\beta^T Y(t)))^2 - \sigma^2]\right) = 0$$
$$E(L_{2t}) = E\left(\frac{1}{n}\sum_{t=1}^{n}[y(t+1) - g(\beta^T Y(t))]\right) = 0. \tag{23}$$

Therefore $E(L_t) = 0$.

Under the alternative hypothesis, $\dot{m}^T$ is not a zero vector, so:

$$E(L_{1t}) = \mathrm{E}\left(\frac{1}{n}\sum_{t=1}^{n}(\dot{m}^T, 1)^T[(y(t+1) - g(\beta^T Y(t)))^2 - \sigma^2]\right) \neq 0. \tag{24}$$

Thus $E(L_t) \neq 0$. Therefore, testing whether d is equal to d^* is equivalent to testing whether $E(L_t)$ is equal to 0, so that the empirical likelihood can be introduced.

Let $\{p_t\}_{t=1}^n$ be the probability of $\{L_t\}_{t=1}^n$, satisfying: $p_t \geq 0, \sum_{t=1}^n p_t = 1$. Under the null hypothesis, the empirical likelihood ratio function is as follows [27, 28]:

$$L(p_t; d, \sigma^2, \beta) = \sup_{d,\sigma^2,\beta}\left\{\prod_{t=1}^n np_t \,\middle|\, \left(\sum_{t=1}^{n} p_t L_t = 0,\ p_t \geq 0, \sum_{t=1}^n p_t = 1\right\}\right. . \tag{25}$$

The empirical likelihood ratio function can be solved by using the Lagrangian multiplier method, the following Lagrangian function is obtained:

$$G = \sum_{t=1}^{n}\log(np_t) - n\lambda\sum_{t=1}^{n}p_t L_t - \phi\left(\sum_{t=1}^{n}p_t - 1\right), \tag{26}$$

where $\lambda \in R, \phi \in R$ are Lagrange operators, and then the minimum value of Lagrangian function G is solved to obtain the optimal solution of p_t as follows:

$$\widehat{p}_t = \frac{1}{n}\frac{1}{1 + x^T L_t}, \tag{27}$$

where x is the solution for the following system of Equation (28).

$$\frac{1}{n}\sum_{t=1}^{n}\frac{L_t}{1 + x^T L_t} = 0. \tag{28}$$

To solve x, you need to define the objective function: $f(x) = \frac{1}{n}\sum_{t=1}^{n}\frac{L_t}{1+x^T L_t}$. x can be solved by the sequential quadratic programing algorithm [30]. The basic idea is to construct a quadratic programing subproblem at the iteration point. And then solving the subproblem and determining a new iteration point are followed. Finally, we repeat the above process until the constraint is satisfied.

Substituting Equation (27) into Equation (25) yields an empirical likelihood ratio statistic:

$$\begin{aligned} R &= -2\log L(p_t; d, \sigma^2, \beta) \\ &= -2\log\left(\prod_{t=1}^{n} n \cdot \frac{1}{n \cdot (1 + x^T L_t)}\right) \\ &= 2\sum_{t=1}^{n}\log(1 + x^T L_t) \end{aligned} . \tag{29}$$

Assumption 1. *Kernel function $K(\mu)$ is a continuous bounded symmetric probability density function and satisfies the first order Lipschitz condition on R. Function $G(\mu)$ has a continuous bounded second derivative on U.*

Assumption 2. *$E(\varepsilon_t | Y = y) = 0, Var(\varepsilon_t) = \sigma^2 < \infty, E(\varepsilon_t^4) \leq C < \infty, E(\varepsilon_t^4 | Y = y) < \infty$, where C is a constant.*

Assumption 3. *For a sufficiently large sample size n, the presence of $G_0 > 0$ makes:*

$$\beta^* = \left|\frac{1}{n}\sum_{t=1}^{n} g'(Y^T(t)\beta)\right| \geq G_0 > 0. \tag{30}$$

Assumption 4. *Explanatory variable Y(t) in the CSI model is uniformly bounded.*

Theorem 1. *Assume the assumptions conditions 1–4 and the null hypothesis in Equation (20) holds, if $n \longrightarrow \infty$, then*

$$R = -2\log L(p_t; d, \sigma^2, \beta) \xrightarrow{L} \chi^2(m + q + 1), \tag{31}$$

where $\chi^2(m + q + 1)$ is a chi-squared distribution with $m + q + 1$ degrees of freedom. Therefore, based on the above theorem results, if the value of statistic R is greater than $\chi^2_{1-\alpha}(m + q + 1)$, there exists a weak sinusoidal signal with random amplitude in the chaotic noise background. Otherwise, the weak sinusoidal signal does not exist.

The proof of the Theorem 1 is detailed in the appendix.

3.2.2. Proposed Algorithm and Pseudocodes for Sinusoidal Signal Detection. The algorithm architecture of detecting weak sinusoidal signals with random amplitude in the chaotic noise based on the profile empirical likelihood ratio method is shown in Figure 3.

In addition, the respective algorithm is shown in Algorithm 1.

4. Numerical Simulation and Analysis

The performance and capability of the CSI model are comprehensively deep validated and verified by the prediction accuracy for detecting weak sinusoidal signals and carried out three different simulation experiments in this section. The chaotic experimental data is generated by the Lorenz system [11] as the chaotic interference. The MSE, the mean absolute error (MAE), and the root-mean-squares error (RMSE) [12–14] are used to evaluate the performances of the proposed algorithm. $y(t)$ is an observational value, $\widehat{y}(t)$

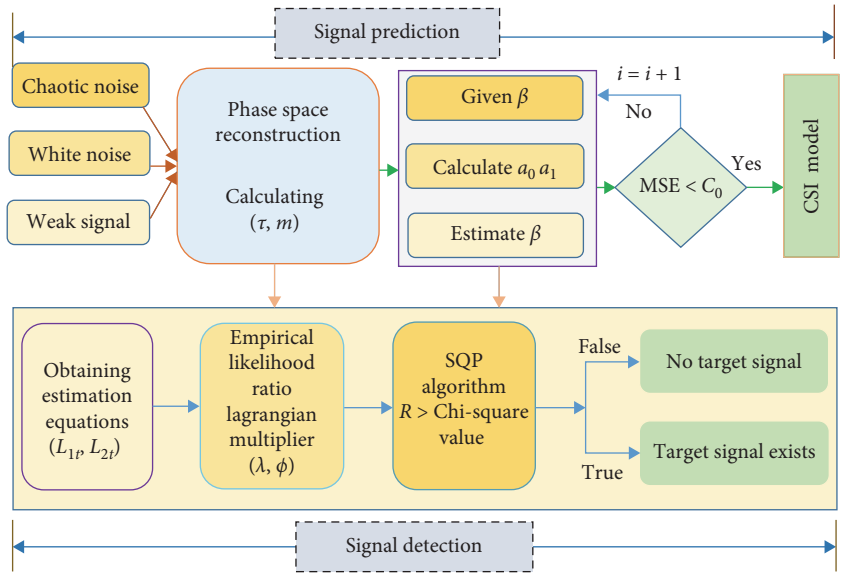

FIGURE 3: Empirical likelihood ratio detection for weak sinusoidal signal.

Input: Observation 1-D data $y(t)$ with the chaotic interference, the parameter delay time τ and the embedding dimension m, constant ζ.

Output: optimal values of the parameters x, β, a_0, a_1, and the values of the statistic R.

Set the β_0

for j to number of epochs do
  Calculate a_0, a_1 with Equations (10) and (11)
  Calculate with Equation (15).
  Repeat steps 2 and 3 until the estimated values of a_0, a_1 and β stable.
end
Set λ_0, ε etc.
for $f(x^{k+1}) - f(x^k) > \varepsilon$ do
  Simplifying the original problem at the point x^k as a quadratic programming problem.
  Set $S^k = S^*$, S^* be the optimal solution of the quadratic programming problem.
  Obtain point x^{k+1} with Equation (28).
  Set $x^* = x^{k+1}, f^* = f(x^{k+1})$.
end
  Set R with Equation (31)
if $(R > \chi^2_{1-\alpha}(m+q+1))$
  the random amplitude sinusoidal signal does exist.
else
  the random amplitude sinusoidal signal does not exist.
end

ALGORITHM 1: Empirical likelihood ratio detection for weak sinusoidal signal.

denotes the predicted value of the proposed model. The performance evaluation formula of the three indicators is as follows:

$$\text{MSE} = \frac{1}{n}\sum_{t=1}^{n}(y(t) - \widehat{y}(t))^2, \tag{32}$$

$$\text{MAE} = \frac{1}{n}\sum_{t=1}^{n}|y(t) - \widehat{y}(t)|, \tag{33}$$

$$\text{RMSE} = \sqrt{\frac{1}{n}\sum_{t=1}^{n}(y(t) - \widehat{y}(t))^2}. \tag{34}$$

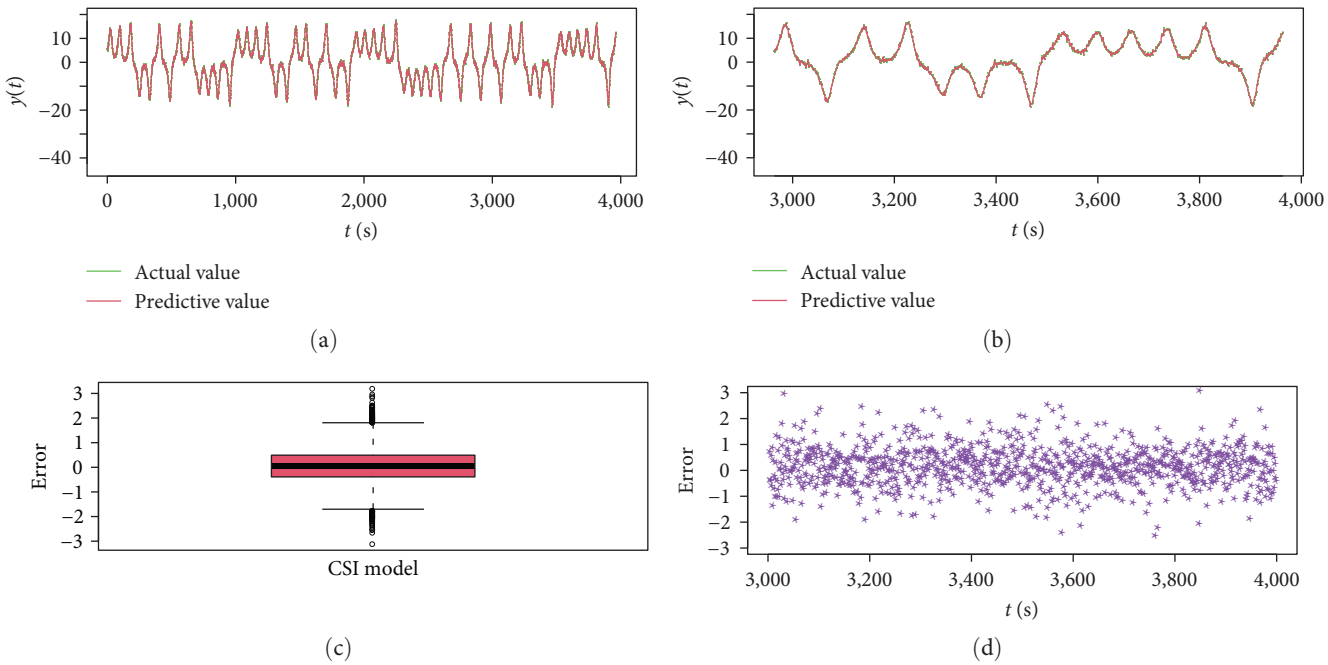

FIGURE 4: Prediction results of chaotic single index (CSI) model: (a) 4,000 points prediction curve; (b) the last 1,000 points prediction curve; (c) 4,000 points error box diagram; (d) the last 1,000 points error curve scattered plot.

Lorenz system is used to simulate the chaotic interference. Its iterative equation is as follows:

$$\begin{cases} \widehat{\eta} = \sigma(y - \eta) \\ \widehat{y} = -\eta z + r\eta - y, \\ \widehat{z} = \eta y - bz \end{cases} \tag{35}$$

where η, y, z is the time function and parameter $\sigma = 10$, $b = 8/3$, $r = 28$. Assuming the initial condition $\eta = 1, y = 1, z = 1$, the sampling time second $t = 0.01$, 10,000 data points are simulated, and the first component η is used as the chaotic 1-D time series data, and 4,000 consecutive points are set as the sample data. The dimension $m = 6$ and the delay time $\tau = 7$ are calculated by the complex auto-correlation method and Cao's method.

4.1. Experiment 1: Effective Evaluation of the CSI Model. A weak random amplitude sinusoidal target signal with $d = 0.7$ for controlling the amplitude and $f_0 = 0.1$ for the sinusoidal signal. To evaluate and verify the effectiveness of the CSI model proposed in this study, the prediction results of CSI model, linear model, and ARIMA are compared. The linear model consists of the input layer of the reconstructed sequence with input phase space, the hidden layer with hidden node of 16 and the output layer of one-step prediction, and an activation function is added between the hidden layer and the output layer. A linear regression model is established to fit the chaotic noise and detect the weak signal under chaotic interference [21]. The ARIMA model only models the input one-dimensional sequence and obtains the prediction results.

The comparison results are shown in Figures 4 and 5. Figure 4(a) shows the prediction curve of the original observation value under the CSI model and the prediction error of detecting a weak sinusoidal signal under chaotic noise. For better visualization, Figure 4(b) only shows the prediction effect of the last 1,000 points, which clearly indicates that the prediction performance is extremely high. As can be seen from Figure 4 the green one-step forward prediction curve fits the red actual curve with very high accuracy, and the mean square error MSE is 0.551. Figures 4(c) and 4(d) show scatter plots of the prediction errors of observation data using chaotic single exponential fitting model. As can be seen from Figure 4, the prediction errors of each point are concentrated near the zero point, which shows that the prediction error of CSI model is very small and the prediction accuracy is very good.

Figure 5(a) shows the prediction curves of 4,000 observed values under the linear model and ARIMA model. The ARIMA model has a poor fitting effect on the actual curve, with a MSE of 0.715, while the linear model has a relatively good fitting effect on the actual curve, with a mean square error of 0.631. Figure 5(b) describes the comparison results of three different methods (CSI model, linear model, and ARIMA model). The closer to a straight line, the better the fitting effect. It can be seen that CSI model is the best, followed by linear model, and finally ARIMA model. In addition, Figure 5(d) shows that the prediction results of linear model and ARIMA model still contain some information, including the information in the original sequence.

The detailed results of the comparison model are summarized in Table 1, which shows the accuracy results of the three evaluation indexes under CSI model, linear model, and ARIMA model.

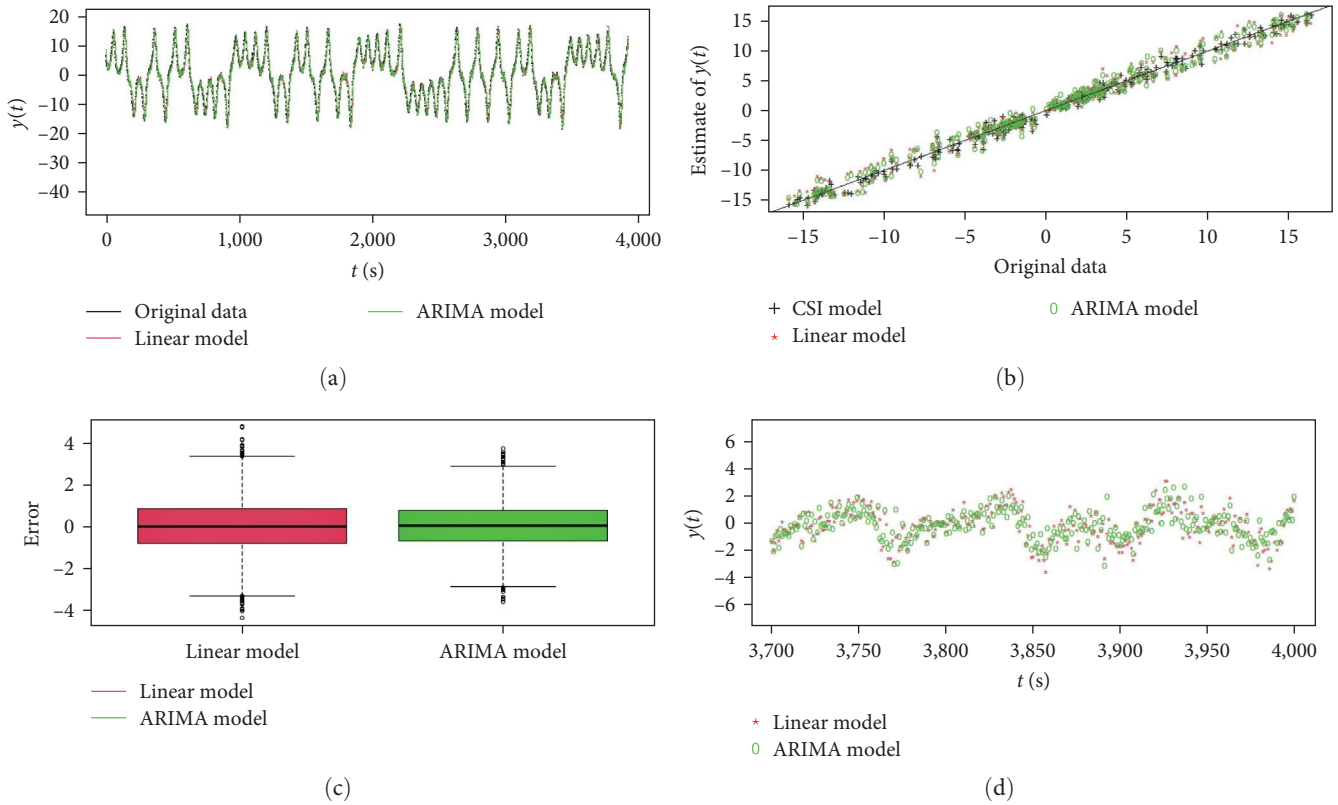

Figure 5: Linear and ARIMA model prediction results: (a) prediction curve; (b) predictive comparison of the CSI model, linear model and ARIMA model; (c) 4,000 data points box plot; (d) 300 data points error plot.

Table 1: Comparison of different prediction models.

MODEL	MSE	MAE	RMSE
CSI model	**0.551**	**0.567**	**0.740**
Linear model	0.631	0.617	0.794
ARIMA model	0.715	0.67	0.846

Bold values signify the result advantage of our model.

It can be seen from Table 1 that, compared with the linear model and ARIMA model, the CSI model proposed in this study has a smaller MSE, MAE, and RMSE of the CSI model than the linear model and ARIMA model, indicating that the CSI model is more effective in predicting the submerged chaotic noise signal. Table 1 illustrates the advantages of the proposed CSI model from the prediction results. The proposed CSI model with profile empirical likelihood ratio exhibits more outstanding predictability and capability than the simple linear model and ARIMA model for weak signal detection, which adopts the nonparametric locally linear Taylor's expression and SQP algorithm.

4.2. Experiment 2: Compared with the Stochastic Resonance Method. To evaluate the feasibility and effectiveness of the empirical likelihood ratio approach, the proposed method in this study for detecting weak sinusoidal signals with random amplitude is compared with the stochastic resonance method [14]. The amplitude of the weak sinusoidal signal is 0.6, and the frequency of the sinusoidal signal is 0.1.

When the background interference is only Gaussian white noise, the presented method is compared with the stochastic resonance method. The results are shown in Figures 6(a) and 6(b). In Figure 6(a), the R statistic is greater than the chi-square value of 15.507, so the weak target signal can be detected with our proposed profile empirical likelihood ratio CSI model. It can be easily seen from Figure 6(b) that the target signal of frequency $f_0 = 0.1$ is detected. When Gaussian white noise is used as background noise, both the proposed method and the stochastic resonance method can detect the existence of a weak target signal.

To further demonstrate the superiority of our investigated scheme, the proposed empirical likelihood ratio detection method is compared with the stochastic resonance method when the mixed noise with chaotic noise and Gaussian white noise is used as background noise. Our proposed approach is implemented by profile least squares and locally linear techniques with R codes. The result of detecting weak harmonic signal is shown in Figure 6(c), R statistic is greater than the chi-square value of 15.507, so the presence of a weak target signal can be detected. The spectrum of the observed signal after stochastic resonance processing is shown in Figure 6(d), but the presence of a weak target signal cannot be detected. When the background noise is the mixed noise of chaotic noise and Gaussian white noise, the proposed method can detect the existence of the target signal, but the stochastic resonance method cannot. The comparison is clear to attain satisfactory results for detecting tasks of hybrid interference. It

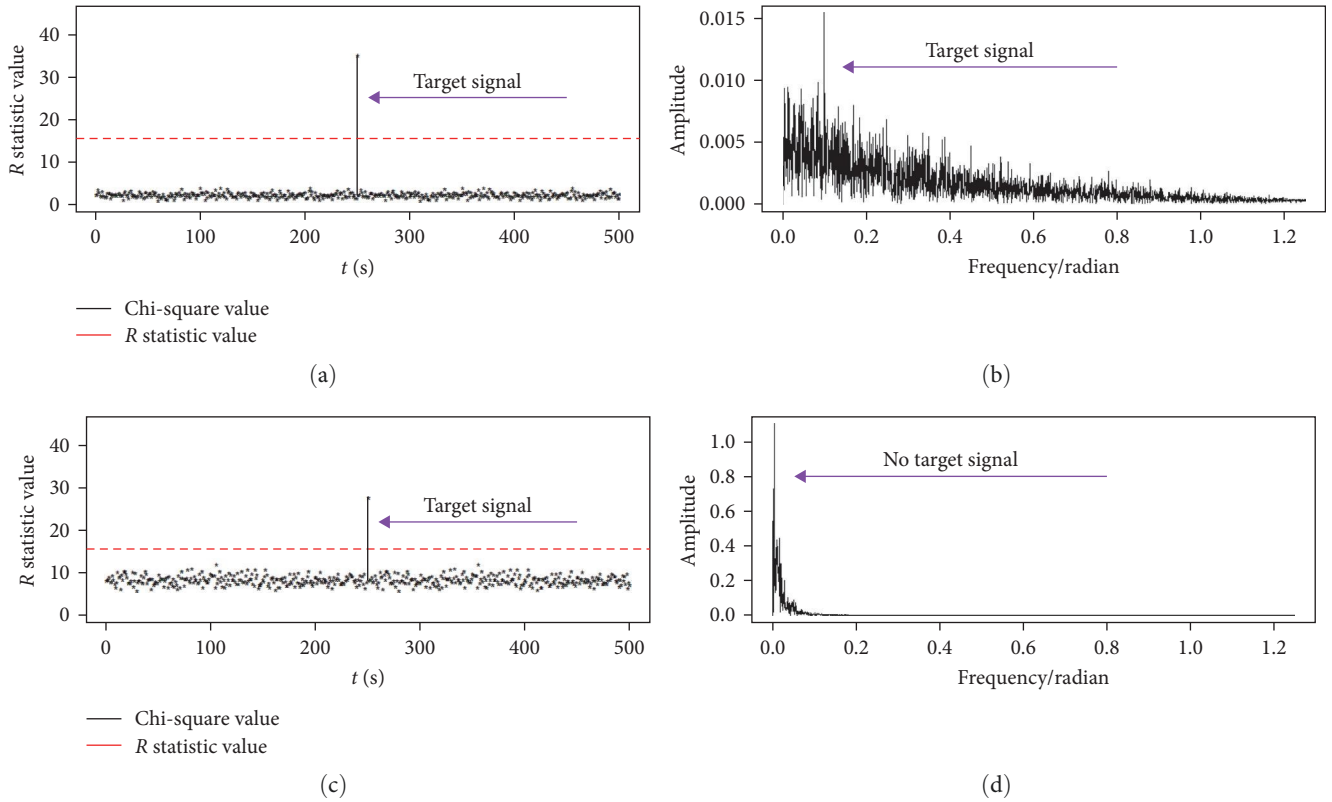

FIGURE 6: Gaussian white noise interference scenario: (a) results of empirical likelihood ratio detection method (the CSI model); (b) results of stochastic resonance detection. Chaotic noise and Gaussian white noise hybrid scenario: (c) results of empirical likelihood ratio detection method (the CSI model); (d) results of stochastic resonance detection.

indicates that the capability of the proposed CSI model to detect the existence of weak sinusoidal signals under chaotic interference is superior to that of stochastic resonance detection.

4.3. Experiment 3: Compared with Neural Network and Breusch–Pagan Test Methods. To further validate the stability and robustness of the presented model, we build the chaotic observational signals with different values of useful target signals and add white noise and chaotic interference to the target signal in the source field. To highlight the exceptional assessment under the target signal environment, the d values with the range of 0.1–1 are set according to different real situations and conditions. The frequency of the weak sinusoidal signal is $f_0 = 0.1$. To verify the effect of the empirical likelihood ratio method for detecting weak sinusoidal signals, the back propagation (BP) neural network method and the Breusch–Pagan test method were compared. In this paper, the structure of BP neural network consists of an input layer, two hidden layers and an output layer. The number of neurons in the hidden layer is 2 and 3, respectively. In addition, the Breusch–Pagan model is used here, which captures the variance of the error term by introducing an additional variable. Specifically, it regresses the square of the residual and the independent variable, and then uses the regression results for statistical test. If the regression results show that the coefficient corresponding to this extra variable

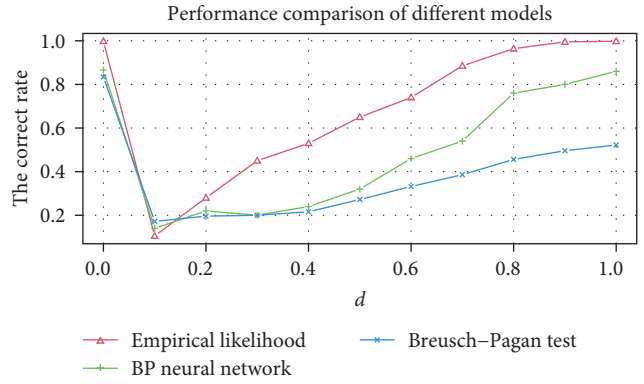

FIGURE 7: Comparison of detection capabilities under different methods (empirical likelihood ratio detection method (the CSI model), BP neural network model, and Breusch–Pagan test model).

is significantly different from zero, then heteroscedasticity can be considered.

The weak sinusoidal signal of different amplitudes was tested 500 times, and the correct rate (correct rate = correct number/total number × 100%) was used as the evaluation indicator. The detection result of different methods is shown in Figure 7 for detecting weak harmonic signals with different amplitudes. It can be seen from Figure 7 that the empirical likelihood ratio detection method has a detection accuracy of 90% when there is no weak random amplitude sinusoidal

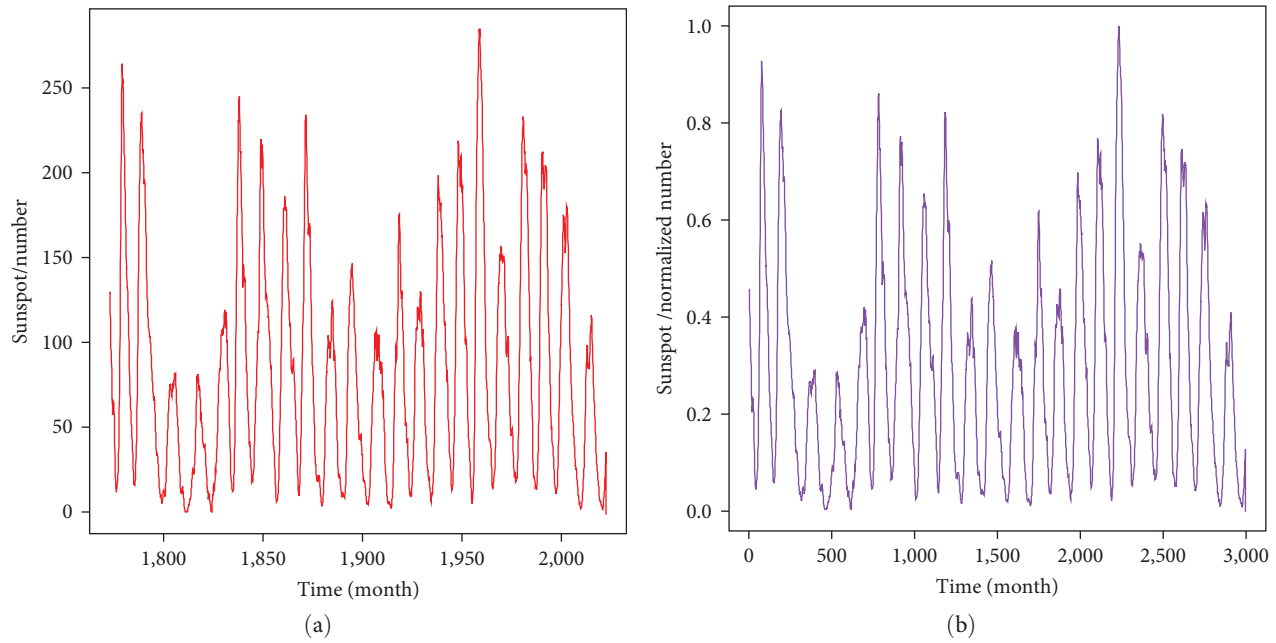

Figure 8: Sunspots: (a) original data and (b) normalized data.

signal, which is greater than the BP neural network detection accuracy rate and less than the Breusch–Pagan test accuracy rate. When there is a weak random amplitude sinusoidal signal, the empirical likelihood ratio detection method has the best detection accuracy compared with other methods. It can be seen from Figure 7 that the empirical likelihood ratio detection method has a detection accuracy of 90% when there is no weak random amplitude sinusoidal signal, which is greater than the BP neural network detection accuracy rate and less than the Breusch–Pagan test accuracy rate. However, the detection results of the three methods are similar at 0 and 0.1. In summary, the proposed scheme for detecting weak signals with a CSI statistical model and empirical likelihood ratio testing method exhibits significant model expression capability than BP neural networks or the Breusch–Pagan model, which applies the local linearity and SQP algorithm.

4.4. Experiment 4: Detection of Weak Sinusoidal Signals under the Sunspot Interference. To further validate the practicability of the proposed scheme in this article, sunspot time series are utilized as chaotic interference. Sunspot datasets can be obtained from the website (http://www.sidc.be/silso/datafiles), and the 13-month smoothed monthly total sunspot number from January 1773 to December 2020 is selected as the chaotic background. Because the sunspot data are relatively large, we normalize the data to keep the original chaotic characteristics unchanged, the results are shown in Figure 8.

To study the detection performance of the proposed CSI model in the sunspot noise, the correct rate is used as the evaluation criterion. The result of different models for detecting weak harmonic signals under different amplitudes is shown in Figure 9. By comparing Figures 7 and 9, we can see that the CSI detection model based on the empirical

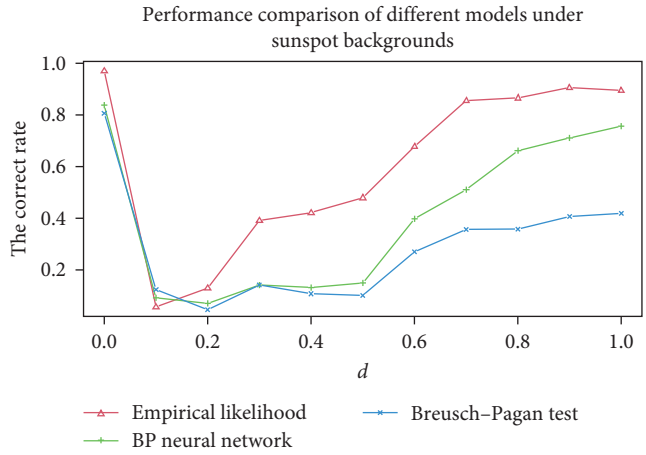

Figure 9: Detection results comparison for different methods under sunspot background (empirical likelihood ratio detection method (the CSI model), BP neural network model, and Breusch–Pagan test model).

likelihood ratio technique has approximately the same effect as the simulated chaotic background with tiny decreasing, and the detection accuracy is about 90% when d is in (0.8, 1), which is greater than the BP neural network method and the Breusch–Pagan test model. Under almost all parameters with different amplitude sinusoidal signals, the empirical likelihood ratio detection method has the best detection accuracy compared with the other methods. However, the detection precision results of the three methods are similar between 0.1 and 0.2. In summary, the proposed CSI model for detecting weak sinusoidal signals with a CSI statistical model and empirical likelihood ratio testing method exhibits significant nonlinear fitting capability compared with the BP neural

network and the Breusch–Pagan test model, and the chaotic noise causes some slight differences in distribution for the training and testing process in target tasks, but the proposed method still achieves effective detection, which is a useful method for weak sinusoidal signal detection in the chaotic background.

5. Conclusion

Weak sinusoidal signals are widely used in bearing and gear fault diagnosis, sea clutter monitoring and many other fields. Therefore, an effective weak signal detection approach must be developed to guarantee the stability and reliability of chaotic systems. Considering this problem, we put forward a novel statistical detection scheme combining the CSI model and empirical likelihood ratio testing, and the weak sinusoidal signal with random amplitude under chaotic background can be detected accurately. This method is simply effective and easy to implement for overcoming the curse of high dimensionality. Based on the characteristics of chaotic background noise, the source data can be reconstructed into multidimensional space, and a hybrid statistical detection model is built creatively by fuzing the CSI model and empirical likelihood ratio technique. The proposed model effectively fits the chaotic background noise and makes the weak sinusoidal signal of random amplitude stand out. According to the heteroscedasticity of such sinusoidal signals, the method based on the empirical likelihood ratio can effectively detect weak signals that are submerged under the background of strong chaos. The empirical likelihood ratio detection approach overcomes the shortcomings of some traditional methods that need to know the overall distribution of the sample and the determination of the estimated variance. The effectiveness and accuracy of the presented model in weak sinusoidal signal detection are essentially and comprehensively investigated by using multiple experimental simulations and scenarios contaminated by the chaotic interference. It can be seen from the simulation's different and deep results that the empirical likelihood ratio method is effective and better than the Breusch–Pagan test and neural network detection for weak sinusoidal signals with random amplitude from chaotic noise. As the amplitude becomes larger, the detection accuracy rate also increases. When the amplitude is greater than 0.6, the detection accuracy rate is as high as 96.0%. Due to the high stability and accuracy, the investigated method exhibits outstanding and robust performance, then it can be extended to the fields of chaotic secure communication, sea clutter processing, biomedical weak signal testing, and rotating machinery fault diagnosis.

In the future, we will continue to explore the influence of the prediction error of the CSI model on the subsequent construction of the detection model to achieve a lower SNR threshold. We will continue to explore the application of the CSI model in signal detection under the sea clutter backgrounds.

Appendix

Theorem A.1. *Assume the assumptions conditions 1–4 and the null hypothesis in Equation (20) holds, if $n \longrightarrow \infty$, then*

$$R = -2\log L(p_t; d, \sigma^2, \beta) \xrightarrow{L} \chi^2(m+q+1). \tag{A.1}$$

Proof. It can be known from Equation (28):

$$\begin{aligned} 0 &= \frac{1}{n}\sum_{t=1}^{n}\frac{L_t}{1+x^T L_t} = \frac{1}{n}\sum_{t=1}^{n} L_t\left[1 - x^T L_t + \frac{(x^T L_t)^2}{1+x^T L_t}\right] \\ &= \frac{1}{n}\sum_{t=1}^{n} L_t - \left(n^{-1}\sum_{t=1}^{n} L_t L_t^T\right)x - n^{-1}\sum_{t=1}^{n}\frac{L_t (xL_t)^2}{1+x^T L_t}. \end{aligned} \tag{A.2}$$

□

Considering the last item in the above formula

$$\begin{aligned} &\left\|\frac{1}{n}\sum_{t=1}^{n}\frac{L_t (x^T L_t)^2}{1+x^T L_t}\right\| \le n^{-1}\sum_{t=1}^{n}\|L_t\|^3\|x\|^2|1+x^T L_t|^{-1} \\ &= o_p\left(n^{1/2}\right). \end{aligned} \tag{A.3}$$

Then know

$$x = \left[\sum_{t=1}^{n} L_t L_t^T\right]^{-1}\left[\sum_{t=1}^{n} L_t\right] + o_p\left(n^{-1/2}\right). \tag{A.4}$$

Theorem proving is similar to literature [23] and can prove:

$$\|x\| = O_p\left(n^{1/2}\right). \tag{A.5}$$

Then

$$\max(1 + x^T L_t) = O_p\left(n^{-1/2}\right)o_p\left(n^{1/2}\right) = o_p(1). \tag{A.6}$$

Taylor expansion of R can be known

$$\begin{aligned} R &= -2\log L(p_t; d, \sigma^2, \beta) \\ &= -2\log\left(\prod_{t=1}^{n} n \cdot \frac{1}{n\cdot(1+x^T L_t)}\right) \\ &= 2\sum_{t=1}^{n}\log(1+x^T L_t), \end{aligned} \tag{A.7}$$

$$\begin{aligned} R &= 2\sum_{t=1}^{n}\log(1+x^{T}L_{t}) \\ &= 2\sum_{t=1}^{n}\left[x^{T}L_{t}-\frac{1}{2}(x^{T}L_{t})^{2}\right]+r_{t}, \end{aligned} \tag{A.8}$$

among them

$$\|r_{t}\| \le \sum_{t=1}^{n}|x^{T}L_{t}|^{3} = o_{p}(1). \tag{A.9}$$

As demonstrated earlier, there is

$$0 = n^{-1}\sum_{t=1}^{n}x^{T}L_{t} - (n^{-1}\sum x^{T}L_{t}L_{t}^{T}x) + o_{p}\left(n^{-1/2}\right). \tag{A.10}$$

That is

$$\sum_{t=1}^{n}x^{T}L_{t} = \sum_{t=1}^{n}(x^{T}L_{t})^{2} + o_{p}(1), \tag{A.11}$$

and so

$$R = \sum_{t=1}^{n}x^{T}L_{t} + o_{p}(1). \tag{A.12}$$

Moreover, the previous one has been proven as follows:

$$x = \left[\sum_{t=1}^{n}L_{t}L_{t}^{T}\right]^{-1}\left[\sum_{t=1}^{n}L_{t}\right] + o_{p}\left(n^{-1/2}\right). \tag{A.13}$$

Substitute it, there is

$$R = \left[\frac{1}{\sqrt{n}}\sum_{t=1}^{n}L_{t}\right]^{T}\left[\frac{1}{n}\sum_{t=1}^{n}L_{t}L_{t}^{T}\right]^{-1}\left[\frac{1}{\sqrt{n}}\sum_{t=1}^{n}L_{t}\right] + O_{p}(1). \tag{A.14}$$

Lemma A.1. *Under the null hypothesis and assumptions 1–4,*

$$\frac{1}{\sqrt{n}}\sum_{t=1}^{n}L_{t}L \xrightarrow{L} N(0,\Omega). \tag{A.15}$$

Lemma A.2. *Under the null hypothesis and assumptions 1–4,*

$$\frac{1}{n}\sum_{t=1}^{n}L_{t}L_{t}^{T}L \xrightarrow{L} \Omega. \tag{A.16}$$

Finally, according to chi-squared distribution conception with the squared sum of independently identically standard normal distribution, we have

$$R = -2\log L(p_{t}; d, \sigma^{2}; \beta)L \xrightarrow{L} \chi^{2}_{(m+q+1)}. \tag{A.17}$$

Therefore, the proof is completed.

Data Availability

The data are available from the corresponding author upon request.

Conflicts of Interest

The authors declare that they have no conflicts of interest.

Acknowledgments

This study was supported by the Natural Science Foundation of Chongqing in China (Grant No. CSTB2023NSCQ-MSX0374).

References

[1] J. K. Yun, N. Weonwoo, and L. Jongsoo, "Multiclass anomaly detection for unsupervised and semi-supervised data based on a combination of negative selection and clonal selection algorithms," *Applied Soft Computing*, vol. 122, Article ID 108838, 2022.

[2] S. E. Sofuoglu and S. Aviyente, "GLOSS: tensor-based anomaly detection in spatiotemporal urban traffic data," *Signal Processing*, vol. 192, Article ID 108370, 2022.

[3] D. Huang, L. Shen, Z. Yu, Z. Zheng, M. Huang, and Q. Ma, "Efficient time series anomaly detection by multiresolution self-supervised discriminative network," *Neurocomputing*, vol. 491, pp. 261–272, 2022.

[4] Y. Chen and M. J. Zuo, "A sparse multivariate time series model-based fault detection method for gearboxes under variable speed condition," *Mechanical Systems and Signal Processing*, vol. 167, Article ID 108539, 2022.

[5] Q. He and J. Wang, "Effects of multiscale noise tuning on stochastic resonance for weak signal detection," *Digital Signal Processing*, vol. 22, no. 4, pp. 614–621, 2012.

[6] K. M. Hock, "Narrowband weak signal detection by higher order spectrum," *IEEE Transactions on Signal Processing*, vol. 44, no. 4, pp. 874–879, 1996.

[7] L. Su, L. Xiong, and J. Yang, "Multi-Attn BLS: multi-head attention mechanism with broad learning system for chaotic time series prediction," *Applied Soft Computing*, vol. 132, Article ID 109831, 2023.

[8] L. Su, M. Yin, and S. Zhao, "PSR-LSTM model for weak pulse signal detection," *Multimedia Tools and Applications*, vol. 82, no. 23, pp. 35853–35877, 2023.

[9] Z. Zhihong and Y. Shaopu, "Application of van der Pol–Duffing oscillator in weak signal detection," *Computers & Electrical Engineering*, vol. 41, pp. 1–8, 2015.

[10] H. Shi, S. Fan, W. Xing, and J. Sun, "Study of weak vibrating signal detection based on chaotic oscillator in MEMS resonant beam sensor," *Mechanical Systems and Signal Processing*, vol. 50-51, pp. 535–547, 2015.

[11] C. Li and L. Qu, "Applications of chaotic oscillator in machinery fault diagnosis," *Mechanical Systems and Signal Processing*, vol. 21, no. 1, pp. 257–269, 2007.
[12] I. G. Silva, W. Korneta, S. G. Stavrinides, R. Picos, and L. O. Chua, "Observation of stochastic resonance for weak periodic magnetic field signal using a chaotic system," *Communications in Nonlinear Science and Numerical Simulation*, vol. 94, Article ID 105558, 2021.
[13] D. Huang, J. Yang, D. Zhou, M. A. F. Sanjuán, and H. Liu, "Recovering an unknown signal completely submerged in strong noise by a new stochastic resonance method," *Communications in Nonlinear Science and Numerical Simulation*, vol. 66, pp. 156–166, 2019.
[14] J. Liu, B. Hu, F. Yang, C. Zang, and X. Ding, "Stochastic resonance in a delay-controlled dissipative bistable potential for weak signal enhancement," *Communications in Nonlinear Science and Numerical Simulation*, vol. 85, Article ID 105245, 2020.
[15] L. Su, L. Deng, W. Zhu, and S. Zhao, "Statistical detecting of weak pulse signal under chaotic noise based on Elman neural network," *Wireless Communications & Mobile Computing*, vol. 2020, Article ID 9653586, 12 pages.
[16] X. Li, W. Zhang, and Q. Ding, "Understanding and improving deep learning-based rolling bearing fault diagnosis with attention mechanism," *Signal Processing*, vol. 161, pp. 136–154, 2019.
[17] L. Su and J. Yang, "Weak pulse signal detection based on the broad learning method under the chaotic background," *Journal of Communications Technology and Electronics*, vol. 67, no. 4, pp. 430–442, 2022.
[18] L. Su, J. Yang, F. Li, and Y. Jiang, "Double-layer robust broad logistic regression for detecting weak pulse signal in chaotic interference," *Digital Signal Processing*, vol. 131, Article ID 103748, 2022.
[19] L. Su, H. Sun, and C. Li, "LL-P-KF hybrid algorithm for detecting and recovering sinusoidal signal in strong chaotic noise," *Acta Electronica Sinica*, vol. 45, no. 4, pp. 837–843, 2017.
[20] D. Ó. Maoiléidigh and A. J. Hudspeth, "Sinusoidal-signal detection by active, noisy oscillators on the brink of self-oscillation," *Physica D Nonlinear Phenomena*, vol. 378-379, pp. 33–45, 2018.
[21] J. Luo, X. Xu, Y. Ding et al., "Application of a memristor-based oscillator to weak signal detection," *The European Physical Journal Plus*, vol. 133, no. 6, Article ID 239, 2018.
[22] O. Sharifi-Tehrani and M. F. Sabahi, "Eigen analysis of flipped Toeplitz covariance matrix for very low SNR sinusoidal signals detection and estimation," *Digital Signal Processing*, vol. 129, Article ID 103677, 2022.
[23] M. Ashourian and O. Sharifi-Tehrani, "Application of semi-circle law and Wigner spiked-model in GPS jamming confronting," *Signal, Image and Video Processing*, vol. 17, no. 3, pp. 687–694, 2022.
[24] O. Sharifi-Tehrani, M. F. Sabahi, and M. Raees Danaee, "Efficient GNSS jamming mitigation using the Marcenko–Pastur law and Karhunen–Loeve decomposition," *IEEE Transactions on Aerospace and Electronic Systems*, vol. 58, no. 3, pp. 2291–2303, 2022.
[25] L. Su, W. Zhu, X. Ling, and S. Zhao, "Weak harmonic signal detecting in chaotic noise based on empirical likelihood ratio," *Wireless Personal Communications*, vol. 126, no. 1, pp. 335–350, 2022.
[26] L. Cao, "Practical method for determining the minimum embedding dimension of a scalar time series," *Physica D: Nonlinear Phenomena*, vol. 110, no. 1-2, pp. 43–50, 1997.
[27] A. Owen, "Empirical likelihood for linear models," *The Annals of Statistics*, vol. 19, no. 4, pp. 1725–1747, 1991.
[28] A. Owen, "Empirical likelihood ratio confidence regions," *The Annals of Statistics*, vol. 18, no. 1, pp. 90–120, 1990.
[29] X. Ma, S. Wang, and W. Zhou, "Statistical inference in massive datasets by empirical likelihood," *Computational Statistics*, vol. 37, no. 3, pp. 1143–1164, 2022.
[30] M. Fesanghary, M. Mahdavi, M. Minary-Jolandan, and Y. Alizadeh, "Hybridizing harmony search algorithm with sequential quadratic programming for engineering optimization problems," *Computer Methods in Applied Mechanics and Engineering*, vol. 197, no. 33–40, pp. 3080–3091, 2008.